Sonolytic decolourisation of Reactive orange 107 dye in the presence of Titanium dioxide and some Rare Earths through adsorption and degradation processes

Pankaj*, Prem Kishore Patnala & Shikha Goyal
Chemistry Department, Dayalbagh Educational; Institute, Agra 282 005, INDIA
e-mail: prof_pankaj99@yahoo.com

Abstract **Sonochemical decolourisation of reactive orange 107 (RO 107), through adsorption and degradation processes, in the presence of ultrasound (US), amorphous TiO_2 and rare earth (REs) ions (La^{+3}, Pr^{+3}, Gd^{+3}, Ce^{+3}) in the aqueous solution, has been examined in the concentration range 8 – 32 mg/L of dye, which was decolorized to about 50% in the presence of US+TiO_2+REs in 50 min. The rate of decolourisation, estimated spectrophotometrically, decreased in different experimental conditions in the order; US+TiO_2+Gd > US+TiO_2+La > US+TiO_2+Ce > US+TiO_2+Pr > US+TiO_2 > US+Gd > US+La > US+Ce > US+Pr > TiO_2 > US respectively. Decrease in the concentration of dye has been fitted to the Langmuir, Freundlich and Temkin adsorption isotherms. Equilibrium results showed that the rate of decolourisation followed pseudo second order kinetics. The mechanism of dye adsorption process was determined from the Webber-Morris model of intraparticle diffusion and Boyd kinetic model. The decolourisation of dye was maximum in systems containing rare earth cations. The adsorption of dye RO 107 enhanced on the surface of TiO_2 through electrostatic attraction, resulting into sand witched structure between TiO_2, REs and Dye molecule.**

Key Words: Ultrasound, Adsorption, RO 107, TiO_2, Rare earths

I. Introduction

Dyes are quite frequently used in textile and leather industries globally, which are also mostly non-biodegradable and toxic, therefore, their presence causes a serious problem even in low concentration. The effluents from the industries may contain upto 15% of the dye used [1]. Due to high solubility, synthetic dyes are common pollutants and may frequently be found in minute quantities in industrial water [2-3], which not only creates an aesthetic problem, but also quite often lead to toxicity and carcinogenicity [4]. Methods like adsorption, filtration, biological methods and flocculation decolourise dyes only incompletely [5]. However, rare earths have recently been shown to facilitate removal of dye [6]. Hence ultrasound in combination with rare earths and an adsorbent surface, TiO_2, has been undertaken to examine the decolourisation of a recalcitrant dye, RO 107.

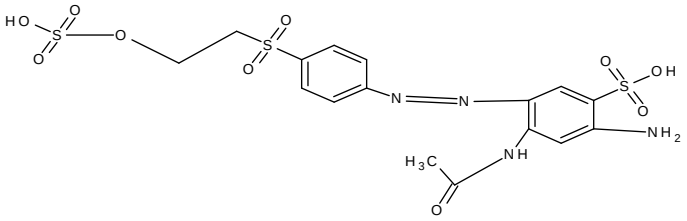

Fig.1. Structure of Reactive Orange 107

Increased mass flow enhances adsorption, which is an efficient and common technique for the removal of dyes from wastewater [7]. Several natural adsorbents such as wood powder [8], fly ash [9], coconut husk [10], lignin [11], banana stalks [12], have been used and reported. Decolourization of dye using TiO_2 in the presence of ultrasound has been found to be better purification method compared to other conventional chemical methods [13-17]. We report here the degradation of Reactive Orange 107 (RO 107) on TiO_2 surface in the presence of ultrasound and rare earth ions for the decolourisation. RO 107 (water solubility 100g/L at 25^0C) [18] is an azo based reactive dye, which binds to textile fibre covalently and thus is highly recalcitrant.[19] Its pKa is 4.1 at 25^0c. Although RO 107 is not a toxic dye but its effect on rats could be lethal (LD50, mg/kg, ≥ 5000) and may cause skin and eye irritation to humans [20].

The rare earth ions initially facilitate complex formation with dye molecules, whereas in the following steps the ultrasound promotes transfer and adsorption of these complexes onto the surface of TiO_2.The nature of adsorption has been examined through Langmuir [30], Freundlich [31] and Temkin [32] adsorption isotherms, whereas, the mechanism has been investigated through Weber–Morris [33] and Boyd [34] models. Ultrasound is known to generate acoustic cavitation [21-24], involving nucleation, growth and collapse of the micro bubbles through

implosion. Inward collapse of bubbles create sites for micro reactors with high temperature (>4000K), pressure (>1000 atm) and mass flow (>500 m/s). Dissolved gases in the water act as the first site of nucleation for cavitating bubbles [25-26]. Such active sites are responsible for the homogenous splitting of water into $^{\bullet}OH$ and $^{\bullet}H$ radicals followed by the formation of a series of free radical reactions within and outside bubbles [27].

II. Experimental Section

Materials and Method

RO 107 [99.9% purity] was received as gift from M/s Spectrum Dyes and Chemicals, Surat, India. Chlorides of Lanthanum, gadolinium, praseodymium and cerium [Indian Rare Earths Ltd, 99.99%], (REs), were kept under vacuum for 2hr before use.

Preparation and characterisation of adsorbent (TiO_2)

Titanium (IV) isopropoxide, Sigma Aldrich (> 97%) was used to synthesise Nanostructured TiO_2 through the hydrolysis in de-ionised water by the known method [28]. 2mL of $(nBuO)_4Ti$ was hydrolysed by pouring into large excess of water (50ml) and sonicating the suspension for 10 minutes. The titania was recovered through filtration and dried in an oven at 70^0C for 12 hrs. The $(n\text{BuO})_4\text{Ti}$, upon hydrolysis in aqueous solution, produced TiO_2 as under;

$$(n\,\text{BuO})_4\,\text{Ti} + \text{H}_2\text{O} \rightarrow \text{Ti(OH)}_4 + 4\text{C}_4\text{H}_9\text{OH} \rightarrow \text{TiO}_2 + 2\text{H}_2\text{O} \qquad (1)$$

The weak and broadened diffraction peaks at small angles were present in XRD spectra (Fig.2), indicating the presence of an amorphous phase with low crystallinity, which was, nevertheless, beneficial to achieve better adsorption of pollutant in the aqueous solution.

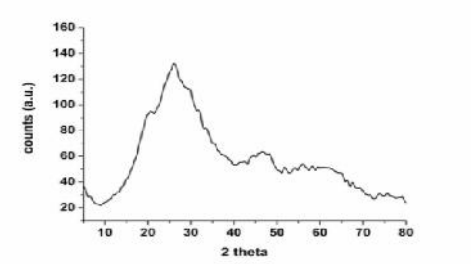

Fig. 2 XRD spectra of TiO_2

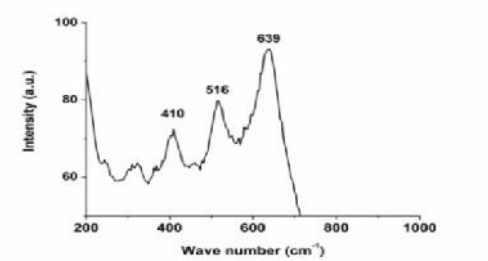

Fig. 3 Raman Spectra of TiO_2

Raman spectra of TiO_2 exhibited bands at 410, 516 and 639 cm^{-1} (Fig.3), but the peaks were less intense and not very sharp indicating partial crystallinity along with amorphous phase. The first two bands were assigned to B_1g and last band was assigned to E_g mode of vibration of the anatase titania phase. From the nitrogen adsorption – desorption isotherm of TiO_2, the average pore diameter, pore volume and BET surface area have been calculated to be 22 – 23 Å, 0.264 cm^3g^{-1} and 475.33 m^2g^{-1} respectively.

Methodology

A stock solution (1000 mg/L) of RO 107 was prepared in tripled deionised water. In 10 mL of dye solution, 0.02ml of TiO_2 and 5mL of 20mg/L RE^{3+} ions were added and this solution was sonicated for 10 to 50 minutes using Vibronics Processor, operating at fixed frequency and power of 20 kHz and 250W respectively. Sonicated solutions were filtered through Sartorius filter disks (grade 393) and were followed through spectrophotometric determination for the concentration of residual amounts of dye using Shimadzu UV-Visible spectrophotometer, 1601PC.

Decolourisation

The % decolourisation of RO 107 has been calculated using the following equation;

$$\%\ \text{Dye Removal} = \frac{C_0 - C_t}{C_t} \qquad (2)$$

Where C_o is the initial concentration of dye (8 mg/L) and C_t is the concentration of dye after time t (50 min).The degradation pathway of RO 107 was studied using electro spray ionization mass spectra (ESI-MS) and experiments were performed on a Water Q- TOF micro Y A-260 (Micromass) tandem quadruple orthogonal TOF instrument, fitted with a lock spray source. The analysis was carried out with capillary voltage of 2220 V, sample cone of 30 V, source temperature of 110ºC and syringe rate of 10µl respectively.

III. Results and Discussion

As can be seen through the spectral changes in different experimental conditions (Fig.4), the combined effect of ultrasound and TiO_2 was additive compared to their application separately. Due to the cavitational effect of US, the de-aggregation of the TiO_2 particles increased, resulting into the enhanced surface area (475.33 m^2g^{-1}) and thus also greater adsorption activity. In the presence of US, the addition of REs shifts the absorption spectral peak of dye from 410 nm to 417 nm, due to the complexation of dye with RE ions. However, in the last condition involving US and TiO_2 in the presence of REs, the decolourisation of dye was maximum due to the enhancement of adsorption of dye on RE-TiO_2 agglomerates as a result of a chemical complexation [29] between RE and the dye. The rare earth ions possess a number of vacant *f*-orbitals, which may accept lone pair of electrons from the N-, O- and S- donor atoms present in the dye molecules. Positively charged complex species (Dye – REs) are transported and get attached to (-) vely charged surface of TiO_2 under the influence of the ultrasound. This increases adsorption initially. However, the cavitational effect of ultrasound and the free radicals, thus produced, subsequently degrade big dye molecules to smaller fragments later.

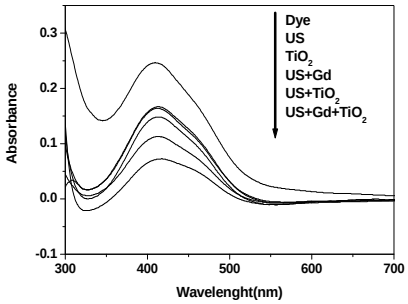

Fig.4 UV-Vis spectra for decolourisation of RO 107 at C_0=8 mg/L; TiO_2= 184 mg/L and RE (Gd^{+3}) =20 mg/L for 50 min

The percent decolourisation of RO 107, under different conditions and time intervals has been given in Table 1 and represented graphically in Fig. 4.

CONDITIONS	% DECOLORISATION AT DIFFERENT TIME INTERVALS (In minutes)				
	10 min	20 min	30 min	40 min	50 min
TiO_2	9.0	9.4	25.9	29.6	31.6
TiO_2+Ce	19.7	25.1	26.7	35.3	36.2
TiO_2+Gd	44.4	45.6	46	48	51
TiO_2+La	40.7	41.9	42.3	43.2	43.6
TiO_2+Pr	20.5	31.6	32.0	32.9	38.2
US	6.5	9.4	27.5	29.2	33.3
US+ TiO_2+Ce	41.1	41.9	44.4	46.5	55.9
US+ TiO_2+La	40.3	54.7	55.5	56.3	65.0
US+ TiO_2+Pr	27.9	30.0	30.4	30.8	31.6
US+Ce	25.1	27.5	28.3	32.0	33.7
US+Gd	34.9	36.2	37	37.4	53
US+La	32	32.5	32.9	35.3	36.2
US+Pr	15.6	30.0	32.5	37.0	38.6
US+TiO_2	27.1	28.3	30.8	32.9	39.0
US+TiO_2+Gd	57.2	59.6	60.4	65.0	69.9

Table 1:% Decolourisation of RO 107 under different conditions and time intervals

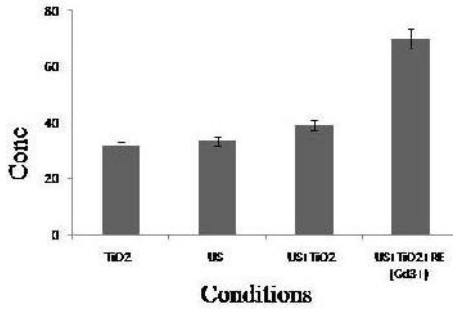

Fig. 5.Graph showing dye decolourisation of RO 107 at C_0=8 mg/L; TiO_2= 184 mg/L and RE (Gd^{+3}) =20 mg/L at different conditions for 50 min

Adsorption Isotherms

The experimental results were fitted into Langmuir, Freundlich and Temkin isotherms. The time at which adsorption reaches equilibrium is 50 min. Isotherm constants of Langmuir, Freundlich, Temkin are based on their regression values (R^2), respectively, that were obtained to fit the isotherm equation.

Langmuir isotherm shows the equilibrium between adsorbate and adsorbent in the system. The linearalised form of Langmuir isotherm [30] is given by the following equation;

$$C_{eq}/q_e = 1/q_m b + C_{eq}/q_m \quad (3)$$

where C_{eq} is the equilibrium concentration of dye (mg/L), q_e is the amount of dye adsorbed at equilibrium (mg/g), q_m is the maximum specific uptake corresponding to the site saturation and b is the Langmuir constant related to energy of adsorption. Langmuir constants q_m and b were calculated from the slope and intercept between $1/q_e$ and $1/C_e$ (Table 2). The essential characteristic of the Langmuir isotherms can be expressed in terms of a dimensionless constant or equilibrium parameter, R_L, which is defined as;

$$R_L = 1/(1 + bC_o) \quad (4)$$

where, C_o (mg/L) is the initial concentration of the dye. From the value of R_L, the nature of adsorption can be interpreted as irreversible (R_L = 0), favourable (0<R_L<1), linear (R_L =1) or unfavourable (R_L > 1). In the present study, the R_L values were found to be between 0 and 1 (Table 2) indicating the favourable adsorption.

Logarithm form of Freundlich adsorption isotherm [31] is given as;

$$\log q_e = \log K_F + n \log C_{eq} \quad (5)$$

where C_{eq} is the equilibrium concentration (mg/L), q_e is the amount of dye adsorbed at equilibrium (mg/g) and K_F and n are constants incorporating all parameters affecting the adsorption process, such as adsorption capacity and intensity respectively. The values of K_F and n were calculated from the intercept and slope of $\log q_e$ and $\log C_{eq}$ (Table 2). Values of 'n', lying between 0 and 10, has been reported to be indicative of favourable isotherm [31], as also found in our study. (Table 2).

Temkin isotherm [32], describes the adsorption potentials of adsorbent and adsorbate and is given by the following equation:

$$q_e = a + b \log C_{eq} \quad (6)$$

where C_{eq} is the concentration of dye at equilibrium (mg/L), q_e is the amount of dye adsorbed per unit weight of adsorbent (mg/g), a & b are constants related to adsorption capacity and intensity of adsorption respectively and were calculated from the intercept and slope of the plot of q_e versus log C_e (Table 2).Table 2, summarises all parameters of the three adsorption isotherms.

Experimental conditions	Langmuir				Freundlich			Temkin	
	q_m (mg/L)	R_L	R^2	K_F (mg/g)	n (Lmg^{-1})	R^2	a (mg/g)	b (Lmg^{-1})	R^2
US+TiO_2	32.73	7.04	0.95	9.87	0.94	0.99	10.29	45.01	0.95
TiO_2	28.49	0.37	0.99	5.73	1.02	0.99	2.43	43.25	0.96
US+TiO_2+Pr	52.46	0.32	0.95	16.82	1.30	0.95	16.35	6.01	0.98
TiO_2+Pr	45.45	0.75	0.92	2.087	0.41	0.99	10.81	188.63	0.93
US+TiO_2+ Ce	68.49	0.28	0.98	23.09	0.28	0.87	22.23	26.89	0.93
TiO_2+ Ce	47.38	0.88	0.96	13.62	0.21	0.96	12.80	105.78	0.92
US+TiO_2+ La	75.18	0.51	0.92	23.98	0.20	0.98	23.54	14.34	0.98
TiO_2+ La	48.49	0.63	0.96	14.64	2.13	0.94	13.93	57.17	0.98
US+TiO_2+ Gd	81.42	0.14	0.92	27.81	0.03	0.97	25.13	3.05	0.97
TiO_2+ Gd	49.42	0.71	0.98	14.88	0.68	0.99	14.71	16.34	0.91

Table.2 Isotherm parameter for the adsorption of RO 107 dye at different experimental conditions

Adsorption kinetics

The kinetics of adsorption of dye on the TiO_2 surface has been found to be pseudo second order and following the equation;

$$t/q_t = 1/h + t/q_e \quad (7)$$

where, q_e is the amount of dye adsorbed at equilibrium (mg/g), q_t is the amount of dye adsorbed at time t (mg/g), $h= kq_e^2$; k is the second order adsorption rate constant (g $mg^{-1}min^{-1}$). The k_2 and q_e values, shown in Table.3, were obtained from the slope and intercept of linear plot of t/q_t versus t.

Experimental conditions	Pseudo second order	
	q_e(cal.) mg/g	R^2
US+TiO_2	14.96	0.99
TiO_2	8.38	0.89
US+TiO_2+Pr	20.15	0.99
TiO_2+Pr	12.08	0.99
US+TiO_2+Ce	21.39	0.99
TiO_2+Ce	13.18	0.74
US+TiO_2+La	22.91	0.99
TiO_2+La	17.15	0.99
US+TiO_2+Gd	24.89	0.99
TiO_2+ Gd	17.28	0.99

Table.3 Kinetic model and other statistical parameters for adsorption of RO 107 dye

Adsorption Mechanism

The mechanism of kinetic adsorption can now be understood by applying the experimental data to the Weber and Morris intra-particle diffusion [33] and Boyd kinetic Models [34].

Weber Morris Kinetic model

The intraparticle diffusion model [30] is expressed by equation (8)

$$q_t = k_p t^{1/2} + c \quad (8)$$

where k_p is the intraparticle rate constant (g mg^{-1} min^{-1}) and c is the intercept (Table 4) obtained from the linear plot of q_t versus $t^{1/2}$. According to Weber Morris (1963), if the plot of q_t against the square was linear and passed through the origin, then intraparticle diffusion would have been the sole rate limiting step. But since the linear plot did not pass through the origin, there was some degree of boundary layer control and intraparticle diffusion was not the rate limiting step.

Boyd –Kinetic Model

Boyd kinetic model [34] is given by the equation (9)

$$Bt = -0.4977 - \ln(1 - F) \quad (9)$$

where $F = q/q_e$, represents the fraction of dye adsorbed at any time t, Here q_e represents amount of dye adsorbed at equilibrium (mg/g) and q represents the amount of dye adsorbed at any time t(min) and Bt is a mathematical fraction of F.

The linear plot of Bt versus t can be employed to test whether sorption was controlled by film diffusion or particle diffusion. A straight line passing through origin indicates that the slowest step in the adsorption process would be intraparticle diffusion and if otherwise, the adsorption would proceed through film diffusion. In our studies, the plots were linear but did not pass through the origin as predicted from intercept 'c' (Table 3) and therefore the adsorption process was controlled only by the film diffusion.

Experimental conditions	Weber and Morris Intraparticle diffusion Model			Boyd Kinetic Model	
	K_p	C	R^2	C	R^2
US+TiO_2	2.88	10.54	0.97	1.09	0.78
TiO_2	0.97	2.34	0.92	0.33	0.94
US+TiO_2+ Pr	0.32	16.21	0.86	0.62	0.85
TiO_2+ Pr	0.15	7.503	0.87	0.2	0.86
US+TiO_2+ Ce	0.33	16.84	0.96	0.74	0.97
TiO_2+ Ce	0.16	9.091	0.94	0.4	0.82
US+TiO_2+ La.	0.65	18.34	0.92	1.05	0.91
TiO_2+ La	0.17	16.30	0.98	1.0	0.96
US+TiO_2+Gd	0.98	22.47	0.98	1.06	0.98
TiO_2+ Gd	0.65	17.65	0.93	1.39	0.92

Table. 4 Intraparticle diffusion and liquid film diffusion rate constants coefficients

For the determination of the sonolytic degradation pathway of RO 107 and identification of possible intermediate products, the sample was sonicated for 2 hr and examined immediately by Electrospray ionization mass spectrometer (ESI-MS). Major intermediates during the degradation process were proposed by using m/z values of the mass spectra. The ESMS analysis showed peaks at m/z values 106, 187, 201, 369, 383, 465, 506 and the possible matching structures for above mass values have been proposed in scheme 1, through two different paths.
The first path of sonochemical degradation of RO 107 involves the dehydrogenation of parent molecule with the generation of product having mass (m/z =520), followed by the removal of ketone group and ethanamine, forming products with masses (m/z=506) and (m/z=465) respectively. The addition of hydroxyl radical to an azo bond gives products with m/z values 278, 187 and m/z 383, respectively, followed by removal of sulphonyl group of fraction with m/z value 187 to form benzene 1,4 diamine(m/z = 106),followed by the decomposition of benzene 1,4 diamine to form 2Z-but-2-ene(m/z=55.12) and further decomposed to form prop1-ene(m/z=43.11). The second path in scheme 1 is proposed to begin with the removal of sulphonyl group leading to formation of an intermediate with mass (m/z=383) and followed by the deamination to form a product with mass (m/z=369). Further degradation takes place by the attack of hydroxyl radical at azo bond to form a product with mass (m/z=278) and 2-[(4-aminophenyl) sulfonyl] ethanol with mass (m/z=201), followed by subsequent degradation using hydroxyl radical to form 4 methyl aniline with mass (m/z=106.19) and further it is degraded to form prop1-ene (m/z=43.11).

Sonochemical Degradation Pathway of RO 107

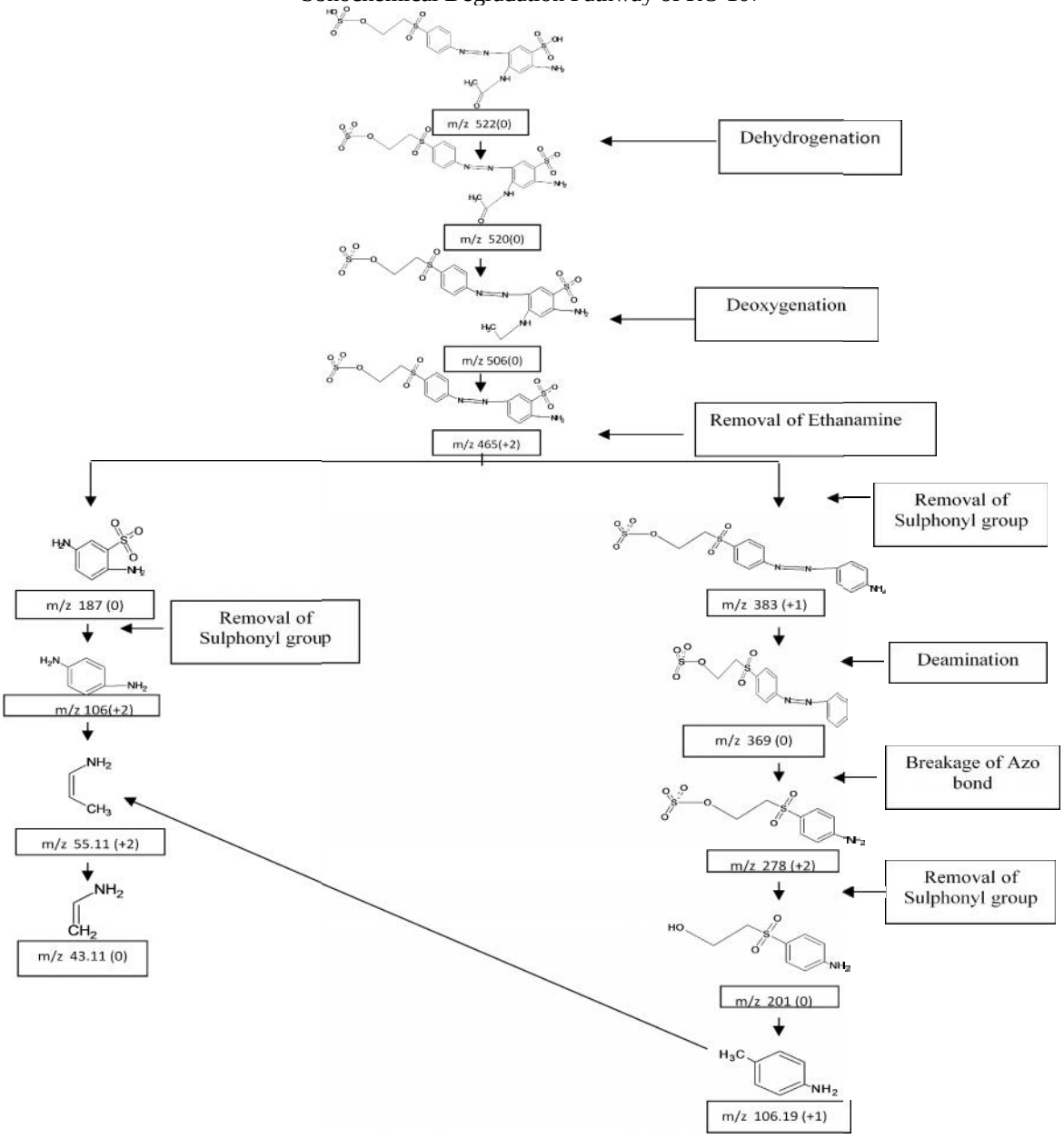

Raman Analysis

Amine NH deformation Vibrations for Amines: Raman spectra of RO 107 recorded after sonicating the solution alterered slightly results in NH deformation of moderate IR bands and weak Raman bands. Particularly in the far IR regions ranging from 1320 - 1345 cm^{-1}, a new peak of medium weak intensity at 1320-1342.5 cm^{-1}, and in the far IR regions ranging from 1280 – 1320 cm^{-1},a new peak of medium weak intensity subdued at 1290 cm^{-1} corresponds to medium weak C-N bond[35] stretching indicates the presence of amine intermediate species. This indicates the breaking of azobond and formation of amine intermediates (Fig.6), This is in conformity with our conclusions in the comparative LC-MS pattern.

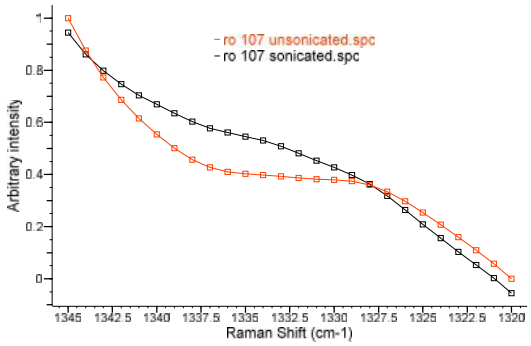

C-N 1345-1320 medium weak stretching.

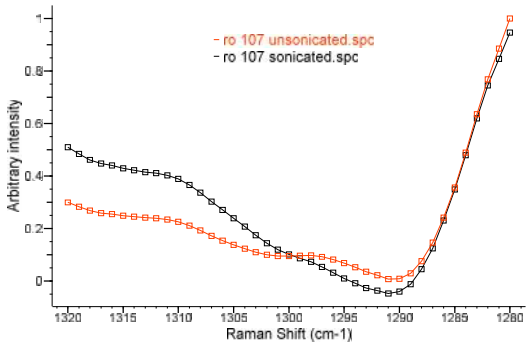

C-N 1320-1280 Medium Strong Stretching.

Fig. 6.Raman Analysis of RO 107

IV. Conclusion

From the results of our study, the 50 % decolourisation of RO 107, in the presence of ultrasound, TiO_2 and Rare earths occured in 50 mins. The degradation proceeds through following three steps; (i).complexation of dye molecule with REs (ii).Migration of RE-Dye complex from the bulk to the surface of TiO_2 and subsequent adsorption and finally (iii).Sonochemical degradation of dye molecule as a result of ultrasonic cavitation and subsequent formation of free radicals H• and •OH in aqueous medium leading to the mineralisation of dye. Adsorption followed all the adsorption isotherms well, but the Langmuir and pseudo second-order kinetic models gave better explanation of the adsorption processes involved in the decolourisation of sample solution. RE-TiO_2 had higher adsorption capacity (q_m) than TiO_2 alone, both in the absence and presence of ultrasound. Boyd kinetic model plot confirmed that the external masss transfer was the slowest step in the adsorption process. LC-MS studies shows that RO107 dye was only partly degradaed sonolytically through the evolution of Prop-1-ene and the formation of amines was conformed by Raman analysis.

Acknowledgement

Authors acknowledge DAE – BRNS for the financial support. PKP is grateful to BRNS and SG to CSIR for SRF.

References

[1] I.Arslan, I.A.Balcioglu, and D.W. Bahnemann, "Heterogeneous photocatalytic treatment of simulated dyehouse effluents using novelTiO2-photocatalysts," Appl.Catal.B.Environ., vol.26, no.3, pp.193-206, 2000.
[2] T.Robinson, G.McMullan, R.Marchant, and P.Nigam, "Remediation of dyes in textile effluent: a critical review on current treatment technologies with a proposed alternative," Bioresour.Technol., vol.77, no.3, pp.247–255, 2001.
[3] I.M.Banat, P.Nigam, D.Singh and R.Marchant, "Microbial decolourisation of textile-dye-containing effluents: A review," Bioresour.Technol., vol.58, no.3, pp. 217-227, 1996.
[4] N.Dhaneshavar,M.Ayazloo,A.R.khataee, and M.Pourhassan,"Biological decolorization of dye solution containing Malachite Green by microalgae Cosmarium sp," Bioresour.Technol., vol.98,no.6, pp.1176-1182, 2007.
[5] O.Legrini, E.Oliveros, and A.M. Braun, "Photochemical processes for water treatment," Chem.Rev., vol.93, no.1, pp.671–698, 1993.
[6] S.Goyal, P.K.Patnala, and Pankaj.Srivastava, "Sonochemical Degradation of Acidic, Reactive and Basic Textile Dyes in the presence of Rare Earths [Lanthanum and Praseodymium]," Int. J.Env. Eng. Manag., vol.3, pp.268-271, 2012.
[7] E.Lorenc-Grabowska, and G.Gryglewicz, "Adsorption characteristics of Congo red on coal-based mesoporous activated carbon," Dyes.Pigm., vol.74, no.1, pp.34-40, 2007.
[8] M. Ozacar and I. A. Sengil, "Adsorption of Metal Complex Dyes from Aqueous Solutions by Pine Sawdust," Bioresour.Technol., vol.96, no.7, pp.791-795, 2005.
[9] B.Acemioglu, "Adsorption of congo red from aqueous solution onto calcium-rich fly ash," J.Colloid.Interf.Sci., vol.274, no.2, pp.371–379, 2004.
[10] I.A.Tan, A.L.Ahmad, and B.H.Hameed, "Adsorption of basic dye on high-surface-area activated carbon prepared from coconut husk: equilibrium, kinetic and thermodynamic studies," J.Hazard. Mater., vol.154, no.1-3, pp.337-346, 2008.
[11] C.M.Luis, M.D.Maria, M.J.Rodriguez, and R.J.Juan, "Lignin-based activated carbons for adsorption of sodium dodecylbenzene sulfonate: Equilibrium and kinetic studies," J.Colloid.and.Interface.Sci., vol.332, no.1, pp.39-45, 2009.
[12] J.M.Salman, and B.H.Hameed,"Removal of insecticide carbofuran from aqueous solutions by banana stalks activated carbon," J. Hazard. Mater., vol.176, no.1-3, pp.814-819, 2010.
[13] J.M. Salman, and B.H. Hameed, "Removal of insecticide carbofuran from aqueous solutions by banana stalks activated carbon," J. Hazard. Mater., vol.176, no.1-3, pp.814-819, 2010.
[14] A.L.Linsebigler, G.Lu, Jr.Yates, and J.T, "Photocatalysis on TiO2 surfaces — Principles, mechanisms, and selected results," Chem.Rev., vol.95, no.3, pp.735–758, 1995.
[15] M.R.Hoffman, S.T.Martin, W.Choi, and D.W.Bahnemann, "Environmental application of semiconductor photocatalysis," Chem.Rev., vol.95, no.3, pp.69-96, 1995.
[16] S. Meriç, H.Elçuk, and V.Belgiorno, "Acute toxicity removal in textile finishing wastewater by Fenton's oxidation, ozone and coagulation-flocculation processes," Water.Res., vol.39, no.6,pp.1147-1153, 2005.
[17] M.Anpo and M.Takeuchi, "The design and development of highly reactive titanium oxide photocatalysts operating under visible light irradiation," J.catal., vol.216, no.1-2, pp.505–516, 2003.
[18] D.Chatterjee, and S. Dasgupta, "Visible light induced photocatalytic degradation of organic pollutantsV," J.Photo-chem. Photobiol. C., vol.6, no.2-3, pp.186-205, 2005.
[19] http://alfaindustries.com/dyes/vsseries/gyellow-rnl-msds.pdf.
[20] Z.Aksu, and F.Gonen, "Biosorption of phenol by immobilizedactivated sludge in a continuous packed bed: prediction of breakthrough curves," Process. Biochem., vol.39, no.5, pp. 599-613, 2004.
[21] http://alfaindustries.com/dyes/vsseries/gyellow-rnl-msds.pdf.
[22] A.M.Basedow, and K.H.Ebert, "Ultrasonic degradation of polymers in solution," Adv.Polym.Sci., vol. 22, pp.83-148, 1977.
[23] A.Henglein, "Sonochemistry: Historical developments and modern aspects," Ultrasonics., vol.25, no.1, pp.6-16,1987.
[24] L.H.Thompson, and L.K.Doraiswamy,"Sonochemsitry:Science and Engineering," Ind.Eng.Chem.Res., vol.38, no.4, pp.1215-1249,1999.
[25] Y.G.Adewuyi, "Sonochemsitry: Environemental science and Engineering applications," Ind.Eng.Chem.Res., vol.40, no.22, pp.4681-4715, 2005.
[26] M.H.Priya, and G.Madras, "Kinetic of TiO_2- Catalyzed ultrasonic degradation of Rhodamine Dyes," Ind.Eng.Chem.Res., vol.45, no.3, pp.913-921, 2006.
[27] M.Kubo, K.Matsuoka, A.Takahashi, N.S.Kitakawa, and T.Yonemoto, "Kinetics of ultrasonic degradation of phenol in presence of TiO_2 particles," Ultrason.Sonochem., vol.12, no.4, pp.263-269, 2005.
[28] N.H. Ince, and G.Tezcanlí, "Reactive dyestuff degradation by combined sonolysis and ozonation," Dyes. Pigm., vol.49, no.3, pp.145-153, 2001.

[29] Pankaj. Srivastava, S.Goyal, and Rajesh.Tayade, "Ultrasound-assisted adsorption of reactive blue 21 dye on TiO_2 in the presence of some rare earths (La,Ce,Pr & Gd)," Can.J.Chem.Eng.,vol.92, no.1, pp.41-51, 2014.
[30] C.H.Liang, B.LiF, C.S.Liu, J.L.Lu, and X.G.Wang, "The enhancement of adsorption and photocatalytic activity of rare earth ions doped TiO_2 for the degradation of orange I,"Dyes. Pigm., vol.76, no.2, pp.477–484, 2008.
[31] I.Langmuir, "The constitution and fundamental properties of solids and liquids,"J.Am.Chem.Soc., vol.39, no.9, pp.1848-1906, 1917.
[32] S.Vasudevan, J.Lakshmi, and R.Vanathi, "Electrochemical coagulation for chromium removal: process optimization, Kinetics, isotherms and sludge characterization," Clean.Soil.Air.Water., vol.38, no.1, pp.9-16, 2010.
[33] M.J.Temkin, and V.Pyzhev, "Recent modifications to Langmuir isotherms,"Acta.Physiochim.URRS., vol.12, pp.217-222, 1940.
[34] W.J. Weber, and J.C. Morris, "Kinetics of adsorption on carbon from solution," J.Sanit. Eng. Div. Proceed. Am. Soc. Civil Eng., vol.89, no.2, pp.31-60, 1963.
[35] G.E.Boyd, A.W.Adamson, and L.S.Myers,"The exchange adsorption of ions from aqueous solutions by organic zeolites. Part II. Kinetics," J.Am.Chem.Soc., vol.69, no.11, pp.2836-2848, 1947.
[36] Lei.Zhu, Ghosh.Trisha, Chong.Yeon.Park, Ze.Da.Meng, and Won.ChunOH, "Synthesis of fullerene modified with Ag_2S with high photocatalytic activity under visible light," Chin. J. Nucl., vol.33, pp. 16127-16135, 2012.